Mineralogical Magazine (2022), **86**, 103–111
doi:10.1180/mgm.2021.82

CAMBRIDGE UNIVERSITY PRESS

Article

New arsenate minerals from the Arsenatnaya fumarole, Tolbachik volcano, Kamchatka, Russia. XVII. Paraberzeliite, $NaCaCaMg_2(AsO_4)_3$, an alluaudite-group member dimorphous with berzeliite

Igor V. Pekov[1]*, Natalia N. Koshlyakova[1], Dmitry I. Belakovskiy[2], Marina F. Vigasina[1], Natalia V. Zubkova[1], Atali A. Agakhanov[2], Sergey N. Britvin[3], Evgeny G. Sidorov[4,†] and Dmitry Yu. Pushcharovsky[1]

[1]Faculty of Geology, Moscow State University, Vorobievy Gory, 119991 Moscow, Russia; [2]Fersman Mineralogical Museum of the Russian Academy of Sciences, Leninsky Prospekt 18-2, 119071 Moscow, Russia; [3]St. Petersburg State University, University Emb. 7/9, 199034 St. Petersburg, Russia; and [4]Institute of Volcanology and Seismology, Far Eastern Branch of Russian Academy of Sciences, Piip Boulevard 9, 683006 Petropavlovsk-Kamchatsky, Russia

Abstract

The new alluaudite-group mineral paraberzeliite was found in the Arsenatnaya fumarole, Second scoria cone of the Northern Breakthrough of the Great Tolbachik Fissure Eruption, Tolbachik volcano, Kamchatka, Russia. In the deepest zone of Arsenatnaya, paraberzeliite (holotype) is associated with anhydrite, diopside, hematite, svabite, berzeliite, schäferite, calciojohillerite, magnesioferrite, ludwigite, fluorapatite, powellite, baryte, and rhabdoborite-group and aphthitalite-group members. In the middle zone of the fumarole, paraberzeliite occurs with hematite, calciojohillerite, badalovite, johillerite, nickenichite, tilasite, svabite, fluorophlogopite, sanidine, cassiterite, anhydrite, metathénardite and belomarinaite. Paraberzeliite forms prismatic crystals up to 0.2 mm × 0.2 mm × 1 mm often occurring in open-work aggregates. It is transparent, brown (from light to dark brown, sometimes with purple or red hue) or green (from pale greenish to yellow–green). The mineral is brittle, cleavage was not observed. The Mohs hardness is 3½. D_{calc} is 3.811 g cm^{-3}. Paraberzeliite is optically biaxial (+), $\alpha = 1.718(4)$, $\beta = 1.728(4)$, $\gamma = 1.742(4)$ and $2V_{meas.} = 85(5)°$. The chemical composition (wt.%, electron-microprobe; holotype) is: Na_2O 6.43, CaO 16.65, MgO 11.64, MnO 1.65, CuO 0.06, Fe_2O_3 2.45, V_2O_5 1.10, As_2O_5 59.46, total 99.44. The calculated empirical formula based on 12 O atoms per formula unit is $(Na_{1.20}Ca_{1.71}Mg_{1.66}Mn_{0.13}Fe^{3+}_{0.18})_{\Sigma 4.88}(As_{2.98}V_{0.07})_{\Sigma 3.05}O_{12}$. Paraberzeliite is monoclinic, *C*2/*c*, $a = 12.3143(7)$, $b = 13.0679(5)$, $c = 6.7717(4)$ Å, $\beta = 113.657(7)°$, $V = 998.14(10)$ Å^3 and $Z = 4$. The crystal structure was solved from single-crystal X-ray diffraction data, $R = 0.0349$. Paraberzeliite is isostructural with other alluaudite-group minerals. Its simplified crystal chemical formula is $^{A(1)}Ca^{A(2)'}Na^{M(1)}Ca^{M(2)}Mg_2(^{T}AsO_4)_3$. The idealised formula is $NaCa_2Mg_2(AsO_4)_3$, or, according to the actual nomenclature of alluaudite-group arsenates, $NaCaCaMg_2(AsO_4)_3$. The name paraberzeliite reflects the dimorphism of this alluaudite-group mineral with the arsenate garnet berzeliite, ideally $(Ca_2Na)Mg_2(AsO_4)_3$.

Keywords: paraberzeliite, new mineral, alluaudite group, berzeliite, arsenate, crystal structure, fumarole sublimate, Tolbachik volcano, Kamchatka

(Received 10 July 2021; accepted 30 October 2021; Associate Editor: Ian T. Graham)

Introduction

In this paper, we continue the characterisation of new arsenate mineral species found in the Arsenatnaya fumarole located at the apical part of the Second scoria cone of the Northern Breakthrough of the Great Tolbachik Fissure Eruption 1975–1976, Tolbachik volcano, Kamchatka Peninsula, Far-Eastern Region, Russia (55°41′N, 160°14′E, 1200 m a.s.l.). Nineteen new minerals have been described in the previous articles of this series: yurmarinite $Na_7(Fe^{3+},Mg,Cu)_4(AsO_4)_6$ (Pekov *et al.*, 2014a), two polymorphs of $Cu_4O(AsO_4)_2$, ericlaxmanite and kozyrevskite (Pekov *et al.*, 2014b), popovite $Cu_5O_2(AsO_4)_2$ (Pekov *et al.*, 2015a), structurally related shchurovskyite $K_2CaCu_6O_2(AsO_4)_4$ and dmisokolovite $K_3Cu_5AlO_2(AsO_4)_4$ (Pekov *et al.*, 2015b), katiarsite $KTiO(AsO_4)$ (Pekov *et al.*, 2016a), melanarsite $K_3Cu_7Fe^{3+}O_4(AsO_4)_4$ (Pekov *et al.*, 2016b), pharmazincite $KZnAsO_4$ (Pekov *et al.*, 2017), arsenowagnerite $Mg_2(AsO_4)F$ (Pekov *et al.*, 2018c), arsenatrotitanite $NaTiO(AsO_4)$ (Pekov *et al.*, 2019a), the two isostructural minerals edtollite $K_2NaCu_5Fe^{3+}O_2(AsO_4)_4$ and alumoedtollite $K_2NaCu_5AlO_2(AsO_4)_4$ (Pekov *et al.*, 2019b), anatolyite $Na_6(Ca,Na)(Mg,Fe^{3+})_3Al(AsO_4)_6$ (Pekov *et al.*, 2019c), zubkovaite $Ca_3Cu_3(AsO_4)_4$ (Pekov *et al.*, 2019d), pansnerite $K_3Na_3Fe^{3+}_6(AsO^4)_8$ (Pekov *et al.*, 2020a), badalovite $NaNaMg(MgFe^{3+})(AsO_4)_3$ (Pekov *et al.*, 2020b), calciojohillerite $NaCaMgMg_2(AsO_4)_3$ (Pekov *et al.*, 2021a), and yurgensonite $K_2SnTiO_2(AsO_4)_2$ (Pekov *et al.*, 2021b).

This paper is devoted to a new representative of the alluaudite group. This mineral, with the end-member formula $NaCa_2Mg_2(AsO_4)_3$, is chemically the same as the garnet-supergroup arsenate berzeliite, ideally $(Ca_2Na)Mg_2(AsO_4)_3$ (Grew *et al.*, 2013). For this reason, we have chosen to name the new mineral paraberzeliite,

*Author for correspondence: Igor V. Pekov, Email: igorpekov@mail.ru
†Deceased 20 March 2021

Cite this article: Pekov I.V., Koshlyakova N.N., Belakovskiy D.I., Vigasina M.F., Zubkova N.V., Agakhanov A.A., Britvin S.N., Sidorov E.G., Pushcharovsky D.Yu. (2022) New arsenate minerals from the Arsenatnaya fumarole, Tolbachik volcano, Kamchatka, Russia. XVII. Paraberzeliite, $NaCaCaMg_2(AsO_4)_3$, an alluaudite-group member dimorphous with berzeliite. *Mineralogical Magazine* **86**, 103–111. https://doi.org/10.1180/mgm.2021.82

Table 1. Chemical composition of paraberzeliite.

No.	[1]	[2]	[3]	[4]	[5]
Sample	FMM 96193 = Tolb–5591	Tolb–5879	Tolb–5470	Tolb–5252	
Colour	purplish–brown	dark brown	yellow–green	pale greenish	
Wt.%					
Na_2O	6.43 (6.20–6.75)	6.14	6.72	6.08	5.45
K_2O	–	0.06	0.06	0.90	
CaO	16.65 (16.23–16.84)	15.96	15.03	16.91	19.73
MgO	11.64 (11.14–12.08)	11.70	12.41	12.81	14.18
MnO	1.65 (1.50–1.80)	4.62	1.84	0.49	
CuO	0.06 (0.00–0.45)	0.21	0.26	0.61	
ZnO	–	–	0.12	0.26	
Fe_2O_3	2.45 (2.00–3.06)	1.33	3.54	2.39	
TiO_2	–	–	0.01	0.21	
SiO_2	–	0.10	0.11	0.12	
P_2O_5	–	0.16	0.35	0.73	
V_2O_5	1.10 (0.77–1.53)	0.94	0.97	0.21	
As_2O_5	59.46 (58.54–60.35)	59.05	58.71	58.61	60.64
SO_3	–	0.48	0.28	0.05	
Total	99.44	100.75	100.41	100.38	100
Formula calculated on the basis of 12 O apfu					
Na	1.20	1.13	1.23	1.12	1
K	–	0.01	0.01	0.11	
Ca	1.71	1.62	1.52	1.72	2
Mg	1.66	1.66	1.75	1.81	2
Mn	0.13	0.37	0.15	0.04	
Cu	0.00	0.01	0.02	0.04	
Zn	–	–	0.01	0.02	
Fe^{3+}	0.18	0.10	0.25	0.17	
Ti	–	–	0.00	0.01	
Si	–	0.01	0.01	0.01	
P	–	0.01	0.03	0.06	
V	0.07	0.06	0.06	0.01	
As	2.98	2.93	2.90	2.91	3
S	–	0.03	0.02	0.00	
ΣT	3.05	3.04	3.02	2.99	3
$\Sigma A + M$	4.88	4.90	4.94	5.04	5

[1] holotype (average for seven spot analyses, ranges are in parentheses), [2] Mn-enriched variety, [3] Fe-enriched variety, [4] Mn- and V-depleted variety, [5] $NaCa_2Mg_2(AsO_4)_3$. Dash indicates that the content is below the detection limit. ΣT = Si + P+V + As + S; $\Sigma A + M$ = Na + K + Ca + Mg + Mn + Cu + Zn + Fe + Ti.

from the Greek παρα for 'near' and the dimorphism with berzeliite. According to the nomenclature of alluaudite-group arsenates (Hatert, 2019), the idealised formula of paraberzeliite is written as $NaCaCaMg_2(AsO_4)_3$.

Both the new mineral and its name (symbol Pbzl) have been approved by the IMA Commission on New Minerals, Nomenclature and Classification, IMA2018-001 (Pekov *et al.*, 2018a). The holotype specimen is deposited in the systematic collection of the Fersman Mineralogical Museum of the Russian Academy of Sciences, Moscow with the catalogue number 96193.

Occurrence and general appearance

The general characterisation of Arsenatnaya, the most mineralogically prolific of Tolbachik fumaroles, and data on the mineral parageneses zonation and distribution in this active, hot fumarole have been reported in previous papers (Pekov *et al.*, 2014a, 2018b; Shchipalkina *et al.*, 2020).

Paraberzeliite is a rare mineral found only in several specimens. The sample which became the holotype of the new mineral (Table 1, #1) was collected by us in July 2016 from the deepest, so-called anhydrite zone of the Arsenatnaya fumarole, situated at the depth of 3–4 m from the surface. In July 2017, in the same zone we found a Mn-enriched variety of paraberzeliite (Table 1, #2). Both Fe-enriched and V- and Mn-depleted varieties of the mineral (Table 1, ##3 and 4) were detected in specimens from the lower part of the middle, so-called polymineralic zone (depth of ~2 m from the surface) of the fumarole. Temperatures measured by us using a chromel–alumel thermocouple at the time of collecting (in 2015–2018) in different pockets varied from 360–380°C (middle, polymineralic zone) to 450–490°C (deepest, anhydrite zone). In both zones, paraberzeliite is a minor constituent of sublimate encrustations formed in open space in cracks and cavities (fumarole chambers). The mineral deposited presumably at temperatures not lower than 500°C. It crystallised directly from the gas phase or, more probably, formed as a result of the interaction between hot volcanic gas and basalt scoria which could be a source of Mg and Ca, the components with very low volatilities in such post-volcanic systems (Symonds and Reed, 1993).

In the anhydrite zone, paraberzeliite occurs in crusts mainly consisting of anhydrite with subordinate amounts of diopside, hematite, svabite and garnets of the berzeliite–schäferite series. Other associated minerals here are calciojohillerite, magnesioferrite, ludwigite, fluorapatite (As- and V-bearing variety), powellite, baryte, and rhabdoborite-group and aphthitalite-group members. In the lower part of the polymineralic zone, paraberzeliite is found in thin encrustations, which mainly consist of hematite and the arsenates calciojohillerite, badalovite, johillerite, nickenichite, tilasite and svabite. Also, in this association, fluorophlogopite, sanidine, cassiterite, anhydrite, metathénardite and belomarinaite occur.

https://doi.org/10.1180/mgm.2021.82 Published online by Cambridge University Press

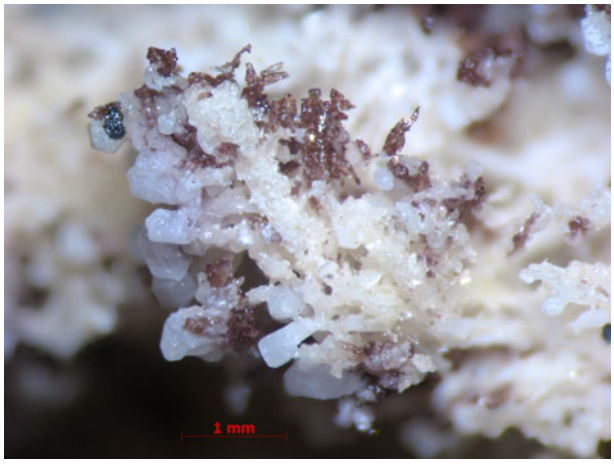

Fig. 1. Open-work clusters of purplish-brown coarse prismatic, distorted crystals of paraberzeliite (holotype, catalogue number 96193) with very pale cream-coloured svabite aggregates and minor iron-black hematite; equant to tabular hexagonal whitish aphthitalite crystals overgrow aggregates of arsenates. Field of view width is 5.7 mm. Photo: I.V. Pekov & A.V. Kasatkin.

Paraberzeliite typically forms coarse, distorted prismatic crystals up to 0.2 mm × 0.2 mm × 1 mm, often occurring in bush-like open-work aggregates, in intimate intergrowths with svabite (Fig. 1), up to 3 mm × 5 mm. Well-formed, sometimes doubly-terminated, multifaceted prismatic crystals (Fig. 2a) up to 0.15 mm long and aggregates thereof (Fig. 2b) were also observed. Paraberzeliite crystals generally contain numerous micro-inclusions of other arsenates and hematite.

Physical properties and optical data

In the holotype specimen, paraberzeliite is purplish-brown (Fig. 1) to brownish-purple, light brown or red–brown. The Mn-enriched variety is dark-brown to brown. The crystals from the polymineralic zone have saturated yellow–green (the Fe-richest variety) to pale greenish colour. Paraberzeliite is transparent, its streak is pale brownish to pale pinkish and the lustre is vitreous. Paraberzeliite is brittle, cleavage was not observed. The fracture is uneven. The Mohs hardness is *ca.* 3½. The density calculated using the empirical formula is 3.811 g cm^{-3}.

In plane polarised transmitted light, paraberzeliite exhibits weak pleochroism with the following absorption scheme: *Y* (greyish purple) > *Z* (very pale yellowish) > *X* (colourless). It is optically biaxial (+), $\alpha = 1.718(4)$, $\beta = 1.728(4)$, $\gamma = 1.742(4)$ (589 nm), $2V_{meas.} = 85(5)°$ and $2V_{calc.} = 81°$. Dispersion of optical axes is very strong, $r < v$. The partially determined optical orientation is $Y = b$.

Raman spectroscopy

The Raman spectrum of the holotype paraberzeliite (Fig. 3) was obtained on a randomly oriented crystal using an EnSpectr R532 instrument with a green laser (532 nm) at room temperature. The output power of the laser beam was ~10 mW. The spectrum was processed using the EnSpectr expert mode program in the range from 4000 to 100 cm^{-1} with the use of a holographic diffraction grating with 1800 lines per cm^{-1} and a resolution of 6 cm^{-1}. The diameter of the focal spot on the sample was ~5 μm. The back-scattered Raman signal was collected with a

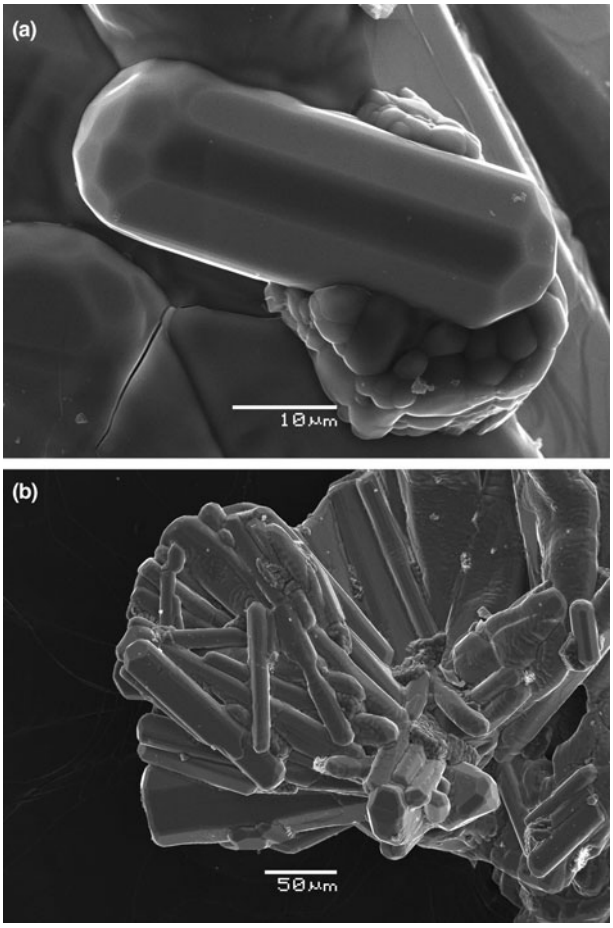

Fig. 2. Multifaceted doubly-terminated prismatic crystal (a) and aggregate of prismatic crystals (b) of paraberzeliite (holotype, catalogue number 96193) overgrowing svabite. SEM (SE) images.

40× objective; signal acquisition time for a single scan of the spectral range was 1500 ms and the signal was averaged over 20 scans.

The bands in the Raman spectrum of paraberzeliite were assigned according to Nakamoto (1986). The bands with maxima at 884, 858 (the strongest band) and 784 cm^{-1} correspond to As^{5+}–O stretching vibrations of AsO_4^{3-} anions and the weak band with maximum at 526 cm^{-1} probably corresponds to Fe^{3+}–O stretching vibrations from the small amount of admixed Fe^{3+}. Bands with frequencies lower than 470 cm^{-1} correspond to bending vibrations of AsO_4 tetrahedra, Mg–O stretching vibrations and lattice modes. The absence of bands with frequencies higher than 900 cm^{-1} indicates the absence of groups with O–H, C–H, C–O, N–H, N–O and B–O bonds.

Chemical composition

The chemical composition of paraberzeliite was studied using a Jeol JSM–6480LV scanning electron microscope equipped with an INCA-Wave 500 wavelength-dispersive spectrometer (Laboratory of Analytical Techniques of High Spatial Resolution, Dept. of Petrology, Moscow State University), with an acceleration voltage of 20 kV, a beam current of 20 nA and a 10 μm beam diameter. The following standards were used: jadeite (Na and Si), $KTiOPO_4$ (K, Ti and P), wollastonite (Ca), olivine (Mg), $MnTiO_3$ (Mn), Cu (Cu), ZnS (Zn and S), FeS_2 (Fe), V (V)

https://doi.org/10.1180/mgm.2021.82 Published online by Cambridge University Press

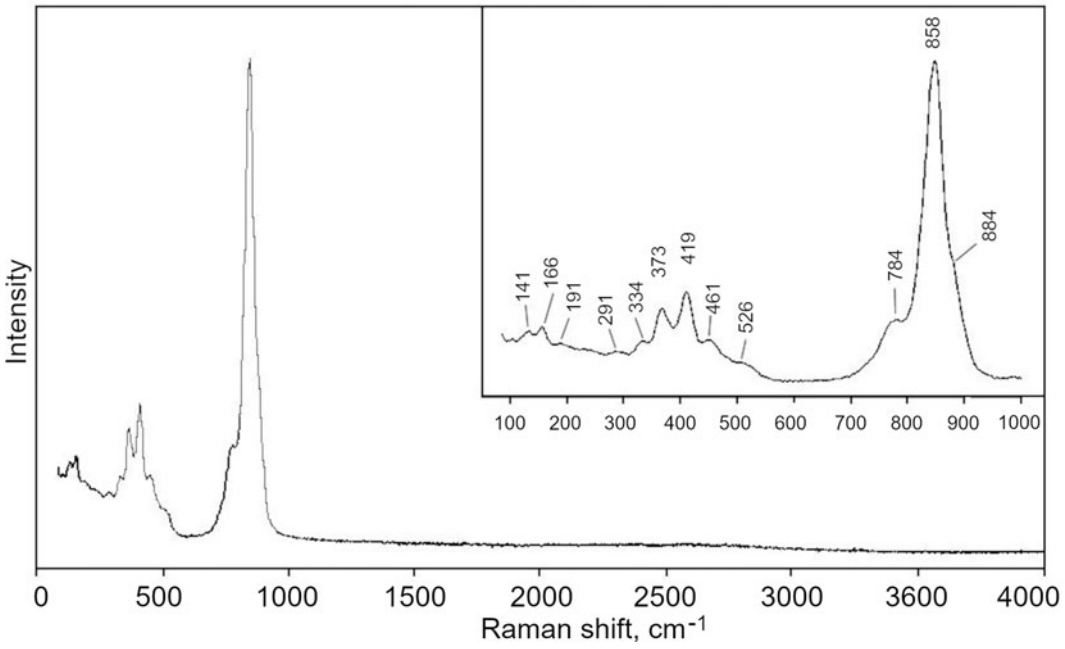

Fig. 3. The Raman spectrum of paraberzeliite.

Table 2. Powder X-ray diffraction data of paraberzeliite.

I_{obs}	I_{calc}*	d_{obs}	d_{calc}**	*h k l*
2	2	8.50	8.539	110
15	17	6.52	6.534	020
1	1	5.938	5.951	11
6	8	5.620	5.640	200
9	8	4.487	4.498	021
15	15	4.406	4.420	111
13	14	4.258	4.269	220
16	16	4.148	4.155	$\bar{2}21\bar{1}$
1	1	4.057	4.063	130
14	15	3.823	3.830	$\bar{3}11$
25	27	**3.642**	3.649	$\bar{1}31$
17	19	**3.606**	3.613	310
2	2	3.337	3.342	$\bar{2}02$
29	36	**3.243**	3.249	$\bar{1}12$
9	10	3.187	3.194	131
22	11, 14	**3.096**	3.104, 3.101	221, 002
34	35, 16	**2.986**	2.992, 2.975	$\bar{3}12$, $\bar{2}22$
22	23	**2.888**	2.891	041
100	100, 45, 10	**2.822**	2.827, 2.820, 2.802	240, 400, 022
14	13	2.780	2.781	$\bar{4}21$
11	12	2.689	2.692	$\bar{4}02$
29	22, 27	**2.658**	2.667, 2.658	112, $\bar{1}32$
5	6	2.585	2.589	420
4	4	2.487	2.489	$\bar{4}22$
2	2	2.415	2.418	$\bar{5}11$
4	2	2.342	2.349	202
5	3, 3	2.332	2.336, 2.332	$\bar{2}42$, 331
5	6	2.306	2.310	132
6	8, 1	2.219	2.223, 2.210	510, 222
1	1, 1	2.190	2.196, 2.189	$\bar{3}13$, $\bar{3}51$
5	6, 2	2.144	2.146, 2.143	350, $\bar{5}31$
2	2	2.076	2.078	$\bar{4}42$
8	5, 1, 12	2.048	2.062, 2.055, 2.048	$\bar{1}52$, 061, $\bar{5}32$
3	2, 2	2.018	2.019, 2.018	$\bar{2}61$, $\bar{4}23$
8	11, 3	1.991	1.991, 1.984	$\bar{3}52$, $\bar{3}33$
3	5	1.959	1.961	$\bar{1}33$
2	3	1.947	1.948	$\bar{6}21$
3	5	1.914	1.915	$\bar{6}22$
6	10, 2	1.884	1.886, 1.883	152, 113

(*Continued*)

https://doi.org/10.1180/mgm.2021.82 Published online by Cambridge University Press

Table 2. (*Continued.*)

I_{obs}	I_{calc}*	d_{obs}	d_{calc}**	*h k l*
4	7, 1	1.855	1.856, 1.853	$\bar{2}43$, 441
8	2, 15	1.835	1.842, 1.837	170, 332
2	4	1.825	1.825	$\bar{2}62$
5	7, 3, 1	1.797	1.798, 1.793, 1.792	$\bar{1}71$, $\bar{5}33$, $\bar{5}51$
3	2, 1, 2	1.780	1.782, 1.780, 1.777	062, $\bar{4}43$, $\bar{4}61$
6	2, 3, 3, 2, 1, 3	1.733	1.735, 1.735, 1.734, 1.731, 1.731, 1.729	$\bar{5}52$, 171, 531, $\bar{6}41$, $\bar{6}23$, $\bar{7}12$
9	4, 11, 5	1.707	1.708, 1.708, 1.703	550, $\bar{6}42$, 422
4	2, 1	1.696	1.696, 1.693	$\bar{3}53$, $\bar{4}62$
11	1, 19	1.676	1.679, 1.677	$\bar{3}14$, $\bar{2}04$
11	2, 2, 18	1.629	1.633, 1.631, 1.629	080, $\bar{1}72$, 640
1	1, 1	1.613	1.614, 1.614	$\bar{1}14$, $\bar{7}13$
5	2, 1, 7	1.597	1.599, 1.597, 1.596	710, 262, $\bar{3}72$
2	3, 1	1.580	1.580, 1.579	081, 621
4	2, 1, 6	1.564	1.567, 1.565, 1.563	$\bar{2}63$, 461, $\bar{2}81$
4	3, 6	1.547	1.552, 1.547	442, 371
8	4, 6, 7, 3	1.539	1.541, 1.540, 1.537, 1.537	512, 172, $\bar{8}02$, $\bar{6}04$
2	3, 1, 3	1.525	1.529, 1.524, 1.523	243, $\bar{1}34$, $\bar{7}33$
2	2, 4, 1	1.510	1.515, 1.511, 1.509	$\bar{5}34$, 730, 024
6	1, 12, 1	1.488	1.489, 1.488, 1.487	$\bar{6}61$, $\bar{4}44$, $\bar{5}71$
1	1, 1, 1	1.473	1.474, 1.473, 1.473	$\bar{6}62$, 333, $\bar{8}21$
2	1, 2, 3	1.453	1.456, 1.454, 1.451	641, $\bar{5}72$, $\bar{7}52$
2	1, 2, 2	1.439	1.442, 1.440, 1.438	$\bar{4}81$, 190, 570
3	1, 1, 5	1.433	1.436, 1.435, 1.431	$\bar{8}23$, $\bar{7}14$, $\bar{3}73$
3	6, 1	1.422	1.422, 1.421	$\bar{1}73$, $\bar{3}54$
2	1, 5	1.409	1.413, 1.410	480, 800
3	11, 1	1.400	1.401, 1.397	044, $\bar{4}82$
2	1, 1, 3	1.372	1.374, 1.373, 1.372	$\bar{5}54$, 372, $\bar{8}41$
4	10	1.361	1.362	204
4	3, 1, 2, 6	1.356	1.356, 1.355, 1.354, 1.354	731, 263, 390, $\bar{5}73$
1	2, 1	1.342	1.342, 1.341	$\bar{8}43$, 282
5	4, 1, 2, 6, 1, 4	1.333	1.334, 1.333, 1.333, 1.332, 1.330, 1.328	552, 224, 173, $\bar{1}92$, $\bar{5}15$, 571
1	1, 2, 1	1.302	1.305, 1.302, 1.301	$\bar{9}32$, $\bar{2}25$, 443

*For the calculated pattern, only reflections with intensities ≥1 are given; **for the unit-cell parameters calculated from single-crystal data; the strongest reflections are marked in bold type.

and GaAs (As). Contents of other elements with atomic numbers higher than carbon were below detection limits.

The chemical compositions of different varieties of paraberzeliite are given in Table 1. The empirical formula of the holotype specimen calculated on the basis of 12 O atoms per formula unit (apfu) is $(Na_{1.20}Ca_{1.71}Mg_{1.66}Mn_{0.13}Fe^{3+}_{0.18})_{\Sigma 4.88}(As_{2.98}V_{0.07})_{\Sigma 3.05}O_{12}$. Taking into account all analyses reported in Table 1 and structural data for the holotype (see below), the simplified formula of paraberzeliite can be presented as $(Na,Ca)(Ca,Na)(Ca,Mn)(Mg,Fe^{3+},Mn)_2(AsO_4)_3$ and the idealised, end-member formula is $NaCaCaMg_2(AsO_4)_3$.

X-ray crystallography and crystal structure determination

The powder X-ray diffraction (XRD) data for holotype paraberzeliite (Table 2) were collected with a Rigaku R-AXIS Rapid II single-crystal diffractometer equipped with cylindrical image plate detector (radius 127.4 mm) using Debye–Scherrer geometry, Co*K*α radiation (rotating anode with VariMAX microfocus optics), 40 kV, 15 mA and 12 min exposure. Angular resolution of the detector is 0.045°2θ (pixel size 0.1 mm). The data were integrated using the software package *osc2Tab* (Britvin *et al.*, 2017). Parameters of the monoclinic unit cell refined from the powder data are: $a = 12.313(8)$, $b = 13.077(3)$, $c = 6.772(4)$ Å, $\beta = 113.75(4)°$ and $V = 998(1)$ Å^3.

Single-crystal XRD studies of the holotype paraberzeliite were performed using an Xcalibur S diffractometer equipped with a CCD detector. A full sphere of three-dimensional data was collected. Intensity data were corrected for Lorentz and polarisation effects. The crystal structure of the new mineral was solved by direct methods and refined using the *SHELX* software package (Sheldrick, 2015). Crystal data, data collection information and structure refinement details are given in Table 3, coordinates and thermal displacement parameters of atoms and bond-valence sums in Table 4 and selected interatomic distances in Table 5. The crystallographic information files have been deposited with the Principal Editor of *Mineralogical Magazine* and are available as Supplementary material (see below).

Unit-cell parameters obtained from the single-crystal XRD data for the Fe-rich variety of paraberzeliite (sample Tolb–5470: Table 1, #3) are: $a = 12.307(17)$, $b = 13.015(14)$, $c = 6.758(11)$ Å, $\beta = 113.52(18)°$ and $V = 993(2)$ Å^3.

Discussion

Paraberzeliite possesses the alluaudite-type structure based on a three-dimensional heteropolyhedral pseudo-framework composed of zig-zag chains of edge-sharing $M(1)O_6$ and $M(2)O_6$ octahedra connected with $T(1)O_4$ and $T(2)O_4$ tetrahedra (Fig. 3a). The *M*-octahedral chains consist of $[M(2)_2O_{10}]$ dimers of distorted $M(2)O_6$ octahedra connected *via* distorted $M(1)O_6$ octahedra isolated from one another (Fig. 4). $T(1)O_4$ tetrahedra share all vertices with the *M*-centred octahedra to form the (010) heteropolyhedral layers, while each $T(2)O_4$ tetrahedron shares three vertices with the MO_6 octahedra of one layer and the fourth vertex with the octahedron of adjacent layer, thus linking the layers to a three-dimensional *M*–*T*–O pseudo-framework. Large-cation positions *A*(1) and *A*(2)' are situated in channels of

https://doi.org/10.1180/mgm.2021.82 Published online by Cambridge University Press

Table 3. Crystal data, data collection information and structure refinement details for paraberzeliite.

Crystal data	
Crystal chemical formula	$(Ca_{0.60}Na_{0.40})_{\Sigma 1.00}(Na_{0.81}Ca_{0.19})_{\Sigma 1.00}$ $Ca_{1.00}(Mg_{1.55}Mn_{0.24}Fe_{0.21})_{\Sigma 2.00}$ $As_{3.00}O_{12}$
Formula weight	579.03
Crystal system, space group, *Z*	Monoclinic, *C*2/*c*, 4
a, *b*, *c* (Å)	12.3143(7), 13.0679(5), 6.7717(4)
β (°)	113.657(7)
V (Å^3)	998.14(10)
F(000)	1097
μ (mm^{-1})	11.711
Data collection	
Data reduction	*CrysAlisPro*, version 1.171.37.34 (Agilent, 2014)
Absorption correction	Gaussian, numerical absorption correction based on Gaussian integration over a multifaceted crystal model
Crystal dimensions (mm^3)	0.10 × 0.06 × 0.05
Diffractometer	Xcalibur S CCD
Temperature (K)	293
Radiation	Mo Kα, λ = 0.71073 Å
θ range (°)	3.118–32.493
Range of *h*, *k*, *l*	−17 → 18, −19 → 19, −9 → 9
Refinement	
No. of measured, independent and observed [$I > 2\sigma(I)$] reflections	9806, 1709, 1506
R_{int}	0.0702
Structure solution	direct methods
Refinement on	F^2
*R*1 and *wR*2 for $I > 2\sigma(I)$	0.0349, 0.0790
*R*1 and *wR*2 for all data	0.0426, 0.0832
No. of parameters refined	99
$\Delta\rho_{max}$, $\Delta\rho_{min}$ (e Å^{-3})	1.192, −1.077
GooF	1.095
Weighting scheme	$w = 1/[\sigma^2(F_o^2) + (0.0348P)^2 + 0.4359P]$ $P = ([\max \text{ of } (0 \text{ or } F_o^2)] + 2Fc^2)/3$

Table 4. Coordinates, equivalent displacement parameters (U_{eq}, Å^2) and bond-valence sums (BVS) for atoms in the structure of paraberzeliite.

Site	Wyckoff	*x*	*y*	*z*	U_{eq}	BVS
A(1)	4b	½	0	0	0.0314(6)	1.55
A(2)'	4e	0	−0.02471(17)	¼	0.0286(8)	0.90
M(1)	4e	0	0.26522(8)	¼	0.0160(2)	2.19
M(2)	8f	0.27788(9)	0.65793(7)	0.36523(14)	0.0143(3)	2.10
T(1)	4e	0	0.72097(4)	¼	0.01224(13)	5.06
T(2)	8f	0.23523(3)	0.89376(3)	0.12924(5)	0.01284(11)	5.01
O(1)	8f	0.4533(2)	0.7033(2)	0.5315(4)	0.0169(5)	2.10
O(2)	8f	0.0989(3)	0.6388(2)	0.2247(5)	0.0254(6)	1.97
O(3)	8f	0.3300(2)	0.66645(19)	0.1089(4)	0.0169(5)	2.05
O(4)	8f	0.1201(2)	0.4129(2)	0.3117(4)	0.0179(5)	2.09
O(5)	8f	0.2278(3)	0.82188(19)	0.3302(4)	0.0174(5)	1.84
O(6)	8f	0.3378(3)	0.50532(19)	0.3925(4)	0.0185(6)	1.91

Bond-valence parameters were taken from Brese and O'Keefe (1991). Bond-valence sums were calculated taking into account cation distribution (see Table 3).

Table 5. Selected interatomic distances (Å) in the structure of paraberzeliite.

A(1)–O(4)×2	2.331(3)	*M*(2)–O(2)	2.036(3)
A(1)–O(2)×2	2.367(3)	*M*(2)–O(3)	2.081(3)
A(1)–O(4)×2	2.574(3)	*M*(2)–O(1)	2.081(3)
<*A*(1)–O>	2.424	*M*(2)–O(5)	2.108(3)
		M(2)–O(6)	2.109(3)
A(2)'–O(6)×2	2.457(3)	*M*(2)–O(5)	2.216(3)
A(2)'–O(6)×2	2.573(3)	<*M*(2)–O>	2.105
A(2)'–O(1)×2	2.699(3)		
A(2)'–O(3)×2	3.151(3)	*T*(1)–O(1)×2	1.678(2)
<*A*(2)'–O>	2.720	*T*(1)–O(2)×2	1.683(3)
		<*T*(1)–O>	1.680
M(1)–O(3)×2	2.314(3)	*T*(2)–O(4)	1.680(3)
M(1)–O(1)×2	2.345(3)	*T*(2)–O(3)	1.681(2)
M(1)–O(4)×2	2.364(3)	*T*(2)–O(6)	1.686(3)
<*M*(1)–O>	2.341	*T*(2)–O(5)	1.688(3)
		<*T*(2)–O>	1.684

two types running through the pseudo-framework parallel to [001] (Fig. 3a). The first channel can be described as a chain of distorted cubes $A(1)O_8$ sharing common faces, and the second as a chain of $A(2)'O_8$ polyhedra connected *via* common edges (Fig. 4). The *M* and *A* cation sites are labelled according to Hatert (2019).

The refinement of the site occupancies in holotype paraberzeliite was performed taking into account electron microprobe data (Table 1, #1); minor admixture of V in the *T* sites was ignored and Na *vs.* Ca were refined for both *A* positions. The refinement of *M*(1) site occupancy with the Ca scattering curve showed 1.01 apfu Ca (probably due to very minor Mn admixture) and was fixed at 1.0 Ca for further refinement. Mg, Fe^{3+} and Mn were assigned to the *M*(2) site with the sum of site occupation factors restrained to be 1.0. The ratio between Na^+ and Fe^{3+} was assumed from the charge-balance requirement, taking into account the only significant heterovalent substitution (see below), which leads to the series with the general simplified formula $Na_{1+x}Ca_2(Mg,Mn)_{2-x}Fe^{3+}_x(AsO_4)_3$.

In paraberzeliite, the *A*(1) site is predominantly occupied by Ca and *A*(2)' by Na. The average *A*(1)–O distance is 2.42 and *A*(2)'–O = 2.72 Å. None of the other sites in the channels known in natural or synthetic alluaudite-type compounds [*A*(1)', *A*(1)", *A*(2), *A*(2)' and *A*(2)": Krivovichev *et al.*, 2013; Đorđevic *et al.*, 2015] are occupied. The *M*(1) site is occupied by Ca [*M*(1)–O = 2.34 Å]. The *M*(2) site is occupied by Mg with admixtures of Fe^{3+} and Mn [*M*(2)–O = 2.11 Å].

The full crystal chemical formula of the structurally studied paraberzeliite crystal can be written as (□ = vacancy): $^{A(1)}(Ca_{0.60}Na_{0.40})_{\Sigma 1.00}$ $^{A(1)'}\square$ $^{A(1)"}\square_2$ $^{A(2)}\square$ $^{A(2)'}(Na_{0.81}Ca_{0.19})_{\Sigma 1.00}$ $^{A(2)"}\square_2$ $^{M(1)}Ca_{1.00}$ $^{M(2)}(Mg_{1.55}Mn_{0.24}Fe_{0.21})_{\Sigma 2.00}$ $^{T}As_{3.0}O_{12}$ (Tables 3 and 5), which is close to the average composition of the holotype sample (Table 1, #1). The structural formula of paraberzeliite simplified to the species-defining constituents is $^{A(1)}Ca^{A(2)'}Na^{M(1)}Ca^{M(2)}Mg_2(^{T}AsO_4)_3 = ^{A}[NaCa]^{M}[CaMg_2](^{T}AsO_4)_3 = NaCaCaMg_2(AsO_4)_3$.

Unlike paraberzeliite, in the structure of its analogue with Mn prevailing in the *M*(2) site, caryinite, ideally $NaCa_2Mn_2(AsO_4)_3$, ^{A}Ca is concentrated in the *A*(1)" site but not in *A*(1). Thus, the simplified structural formula of caryinite is $^{A(1)"}Ca^{A(2)'}Na^{M(1)}Ca^{M(2)}Mn_2(^{T}AsO_4)_3$. Notably, caryinite from a hydrothermal mineral assemblage in the famous Långban skarn deposit in Varmland, Sweden, contains significant admixture of Mg concentrated in the *M*(2) site: $^{M(2)}(Mn_{1.45}Mg_{0.54}Fe_{0.01})_{\Sigma 2.00}$ (Ercit, 1993). Some specimens of paraberzeliite contain up to 0.4 apfu Mn (Table 1, #2) and the existence of a hypothetical isomorphous series between caryinite and paraberzeliite is possible, such as is known for the Långban series between berzeliite $(Ca_2Na)Mg_2(AsO_4)_3$ and manganberzeliite $(Ca_2Na)Mn_2(AsO_4)_3$ (Holtstam and Langhof, 1999); the arsenate garnets are dimorphous with these alluaudite-group minerals. A related pair of alluaudite-group minerals, arseniopleite $NaCaMn_3(AsO_4)_3$ (the sample from the Långban-type deposit Sjö in Sweden was studied: Tait and Hawthorne, 2003) and calciojohillerite

https://doi.org/10.1180/mgm.2021.82 Published online by Cambridge University Press

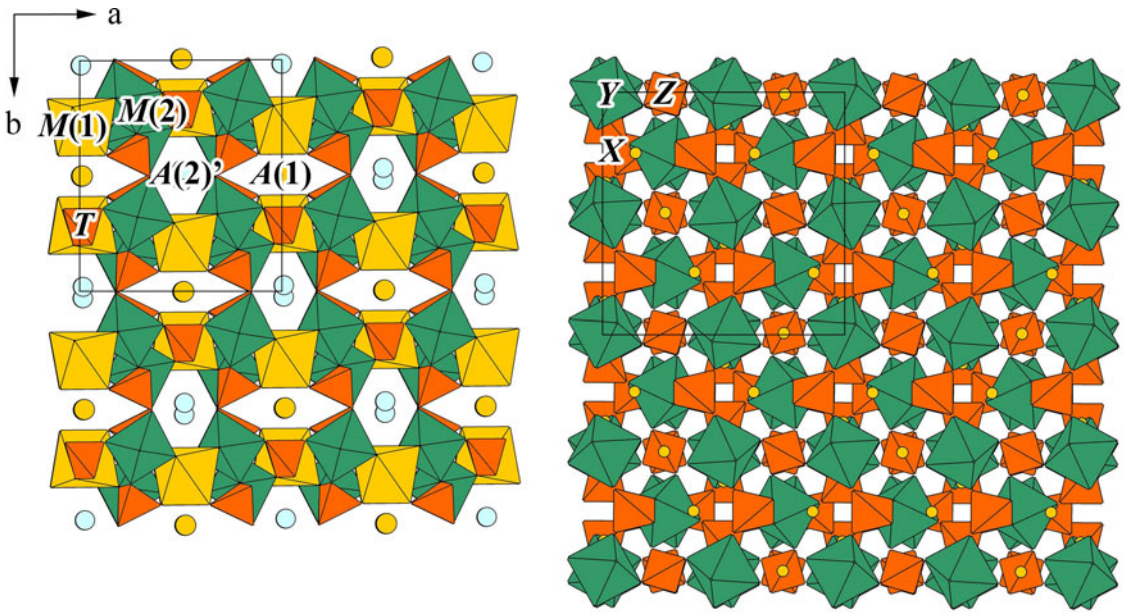

Fig. 4. Crystal structures of dimorphous paraberzeliite (left) and berzeliite (right, drawn based on data of Hawthorne (1976); the *X* site marked as yellow circle contain Ca and Na, *Y* – Mg and *Z* – As^{5+}). Unit cells are outlined.

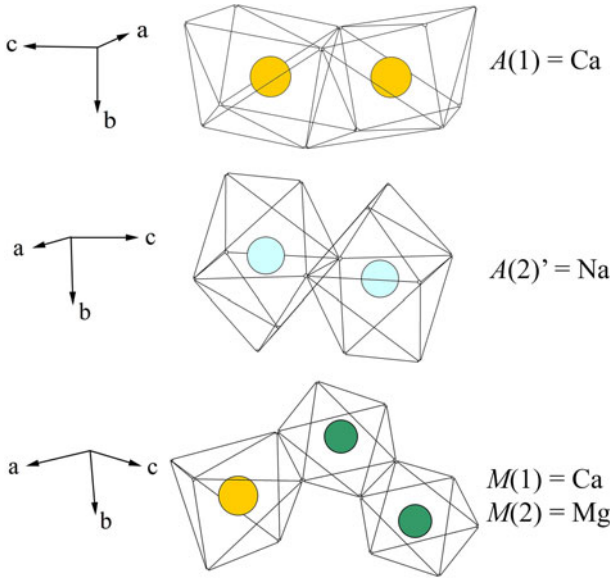

Fig. 5. Motifs of AO_8 and MO_6 polyhedra in the crystal structure of paraberzeliite. Colours of circles showing different cations correspond to Fig. 4, left.

Table 6. Comparative data for paraberzeliite and berzeliite.

Mineral	Paraberzeliite	Berzeliite
Idealised formula	$NaCaCaMg_2(AsO_4)_3$	$(Ca_2Na)Mg_2(AsO_4)_3$
Structure type	Alluaudite	Garnet
Crystal system	Monoclinic	Cubic
Space group	*C*2/*c*	$Ia\bar{3}d$
a (Å)	12.3143(7)	12.355
b (Å)	13.0679(5)	
c (Å)	6.7717(4)	
β (°)	113.657(7)	
V (Å^3)	998.14(10)	1886
Z	4	8
$D_{calc.}$ (g cm^{-3})	3.81	4.07–4.08
Strongest reflections of the powder XRD pattern: *d* (Å) – *I*	3.642–25 3.243–29 3.096–22 2.986–34 2.888–22 2.822–100 2.658–29	5.03–60 3.09–60 2.754–100 2.632–60 2.517–60 1.712–70 1.648–70
Optical data	Biaxial (+) α = 1.718 β = 1.724 γ = 1.742 2V = 85°	Isotropic *n* varies from 1.707 to 1.748, depending on chemical composition
Source	this work	Hawthorne (1976); Anthony *et al.* (2000)

$NaCaMg_3(AsO_4)_3$ (from the Arsenatnaya fumarole: Pekov *et al.*, 2021a), demonstrates the same features of ^{A}Ca distribution: their simplified structural formulae are $^{A(1)"}Ca\ ^{A(2)'}Na^{M(1)}Mn^{M(2)}Mn_2(AsO_4)_3$ and $^{A(1)}Ca^{A(2)'}Na^{M(1)}Mg^{M(2)}Mg_2(AsO_4)_3$, respectively.

The synthetic analogue of the end-member paraberzeliite was reported and dimorphism between alluaudite- and garnet-type synthetic arsenates with the same general formula $NaCa_2M_2^{2+}(AsO_4)_3$ (*M* = Mg, Ni and Co) was discussed by Khorari *et al.* (1997).

The garnet-type structure of berzeliite $^{X}(Ca_2Na)^{Y}Mg_2(^{Z}AsO_4)_3$ is significantly denser compared to that of paraberzeliite. In particular, the distances (Ca,Na)–O in the dodecahedrally coordinated *X* site is 2.47 Å and Mg–O in the octahedrally coordinated *Y* site is 2.10 Å (Hawthorne, 1976). The unit-cell volume of berzeliite is 1886 Å^3 (*Z* = 8), whereas the corresponding, i.e. doubled value of unit-cell volume of paraberzeliite is 998 × 2 = 1996 Å^3. These minerals significantly differ from one another in powder XRD patterns, physical properties including optical data (Table 6) and crystal morphology. Notably, in the Arsenatnaya fumarole, these dimorphs, even though they occur together in the anhydrite zone, clearly differ from one another in colour: paraberzeliite is brown (from light to dark brown, sometimes with purple or red hue) or brownish-purple, whereas berzeliite

https://doi.org/10.1180/mgm.2021.82 Published online by Cambridge University Press

is yellow (from orange- or lemon-yellow to pale yellowish, almost colourless) or bright orange.

Garnets of the continuous isomorphous series berzeliite $(Ca_2Na)Mg_2(AsO_4)_3$ – schäferite $(Ca_2Na)Mg_2(VO_4)_3$ from the Arsenatnaya fumarole have been studied by us in detail (Koshlyakova *et al.*, 2020). Berzeliite from this locality differs distinctly from paraberzeliite in the composition of impurities. Berzeliite contains very few admixed *X* and *Y* constituents; in particular, it is Mn- and Fe-poor (0.1–0.5 wt.% MnO and 0.00–0.5 wt.% Fe_2O_3 that corresponds to 0.01–0.03 apfu Mn and 0.00–0.03 apfu Fe) and the K content in all analyses of these garnets is below the detection limit. Compared to paraberzeliite, berzeliite is Si-enriched: in the majority of samples of this garnet, SiO_2 content varies from 0.4 to 2.0 wt.% (= 0.03–0.17 apfu Si) and in some cases reaches 3.8 wt.% (= 0.35 apfu Si). The Na content in Tolbachik berzeliite is less than 1.0 apfu (in the Si-enriched variety it decreases to 0.70 apfu as a result of the major heterovalent substitution $^{T}Si^{4+} + {}^{X}Ca^{2+} \rightarrow {}^{T}As^{5+} + {}^{X}Na^{+}$), whereas in all the samples of paraberzeliite investigated, the Na content is higher than 1.1 apfu due to the major heterovalent substitution $^{M}Fe^{3+} + {}^{A}Na^{+} \rightarrow {}^{M}Mg^{2+} + {}^{A}Ca^{+}$ [a hypothetic isomorphous series paraberzeliite $NaCaCaMg_2(AsO_4)_3$ – magnesiohatertite $NaNaCa(MgFe^{3+})(AsO_4)_3$ can be suggested]. Correspondingly, the Ca content in berzeliite from Arsenatnaya is higher than 1.95 apfu (typically > 2.0 apfu), whereas in paraberzeliite it is less than 1.75 apfu.

Both berzeliite and paraberzeliite occur in the same paragenesis in the anhydrite zone of the Arsenatnaya fumarole; however, the former is an abundant mineral here, sporadically composing up to 10 vol.% of fumarolic encrustations, whereas the latter is rare and was only detected in small amounts in several specimens. The dense garnet-type structure of berzeliite is probably more stable than the alluaudite-type structure under the high-temperature and low-pressure conditions characteristic of fumarolic systems.

Acknowledgements. We thank referees Anthony R. Kampf and Peter Leverett for their valuable comments. This study was supported by the Russian Science Foundation, grant no. 19-17-00050. The technical support by the SPbSU X-Ray Diffraction Resource Center in the powder XRD study is acknowledged.

Supplementary material. To view supplementary material for this article, please visit https://doi.org/10.1180/mgm.2021.82

References

Agilent Technologies (2014) *CrysAlisPro Software system, version 1.171.37.35*. Agilent Technologies UK Ltd, Oxford, UK.

Anthony J.W., Bideaux R.A., Bladh K.W. and Nichols M.C. (2000) *Handbook of Mineralogy. IV. Arsenates, Phosphates, Vanadates*. Mineral Data Publishing, Tucson.

Brese N.E. and ÒKeeffe M. (1991) Bond-valence parameters for solids. *Acta Crystallographica*, **B47**, 192–197.

Britvin S.N., Dolivo-Dobrovolsky D.V. and Krzhizhanovskaya M.G. (2017) Software for processing the X-ray powder diffraction data obtained from the curved image plate detector of Rigaku RAXIS Rapid II diffractometer. *Zapiski Rossiiskogo Mineralogicheskogo Obshchestva*, **146**(3), 104–107 [in Russian].

Đorđevic T., Wittwer A. and Krivovichev S.V. (2015). Three new alluaudite-like protonated arsenates: $NaMg_3(AsO_4)(AsO_3OH)_2$, $NaZn_3(AsO_4)(AsO_3OH)_2$ and $Na(Na_{0.6}Zn_{0.4})Zn_2(H_{0.6}AsO_4)(AsO_3OH)_2$. *European Journal of Mineralogy*, **27**, 559–573.

Ercit T.S. (1993) Caryinite revisited. *Mineralogical Magazine*, **57**, 721–727.

Grew E.S., Locock A.J., Mills S.J., Galuskina I.O., Galuskin E.V. and Hålenius U. (2013) Nomenclature of the garnet supergroup. *American Mineralogist*, **98**, 785–811.

Hatert F. (2019) A new nomenclature scheme for the alluaudite supergroup. *European Journal of Mineralogy*, **31**, 807–822.

Hawthorne F.C. (1976) Refinement of the crystal structure of berzeliite. *Acta Crystallographica*, **B32**, 1581–1583.

Holtstam D. and Langhof J. (Editors) (1999) *Långban: The Mines, Their Minerals, Geology and Explorers*. Raster Förlag, Stockholm.

Khorari S., Rulmont A. and Tarte P. (1997). The arsenates $NaCa_2M_2^{2+}(AsO_4)_3$ (M^{2+} = Mg, Ni, Co): influence of cationic substitutions on the garnet–alluaudite polymorphism. *Journal of Solid State Chemistry*, **131**, 290–297.

Koshlyakova N.N., Pekov I.V., Zubkova N.V., Agakhanov A.A., Turchkova A.G., Kartashov P.M., Sidorov E.G. and Pushcharovsky D.Yu. (2020) A new solid solution with garnet structure: The berzeliite–schäferite isomorphous series from fumarole exhalations of the Tolbachik volcano, Kamchatka. *Zapiski Rossiiskogo Mineralogicheskogo Obshchestva*, **149**(6), 69–84 [in Russian].

Krivovichev S.V., Vergasova L.P., Filatov S.K., Rybin D.S., Britvin S.N. and Ananiev V.V. (2013) Hatertite, $Na_2(Ca,Na)(Fe^{3+},Cu)_2(AsO_4)_3$, a new alluaudite-group mineral from Tolbachik fumaroles, Kamchatka peninsula, Russia. *European Journal of Mineralogy*, **25**, 683–691.

Nakamoto K. (1986) *Infrared and Raman Spectra of Inorganic and Coordination Compounds*. John Wiley & Sons, New York.

Pekov I.V., Zubkova N.V., Yapaskurt V.O., Belakovskiy D.I., Lykova I.S., Vigasina M.F., Sidorov E.G. and Pushcharovsky D.Yu. (2014a) New arsenate minerals from the Arsenatnaya fumarole, Tolbachik volcano, Kamchatka, Russia. I. Yurmarinite, $Na_7(Fe^{3+},Mg,Cu)_4(AsO_4)_6$. *Mineralogical Magazine*, **78**, 905–917.

Pekov I.V., Zubkova N.V., Yapaskurt V.O., Belakovskiy D.I., Vigasina M.F., Sidorov E.G. and Pushcharovsky D. Yu. (2014b) New arsenate minerals from the Arsenatnaya fumarole, Tolbachik volcano, Kamchatka, Russia. II. Ericlaxmanite and kozyrevskite, two natural modifications of $Cu_4O(AsO_4)_2$. *Mineralogical Magazine*, **78**, 1527–1543.

Pekov I.V., Zubkova N.V., Yapaskurt V.O., Belakovskiy D.I., Vigasina M.F., Sidorov E.G. and Pushcharovsky D.Yu. (2015a) New arsenate minerals from the Arsenatnaya fumarole, Tolbachik volcano, Kamchatka, Russia. III. Popovite, $Cu_5O_2(AsO_4)_2$. *Mineralogical Magazine*, **79**, 133–143.

Pekov I.V., Zubkova N.V., Belakovskiy D.I., Yapaskurt V.O., Vigasina M.F., Sidorov E.G. and Pushcharovsky D.Yu. (2015b) New arsenate minerals from the Arsenatnaya fumarole, Tolbachik volcano, Kamchatka, Russia. IV. Shchurovskyite, $K_2CaCu_6O_2(AsO_4)_4$, and dmisokolovite, $K_3Cu_5AlO_2(AsO_4)_4$. *Mineralogical Magazine*, **79**, 1737–1753.

Pekov I.V., Yapaskurt V.O., Britvin S.N., Zubkova N.V., Vigasina M.F. and Sidorov E.G. (2016a) New arsenate minerals from the Arsenatnaya fumarole, Tolbachik volcano, Kamchatka, Russia. V. Katiarsite, $KTiO(AsO_4)$. *Mineralogical Magazine*, **80**, 639–646.

Pekov I.V., Zubkova N.V., Yapaskurt V.O., Polekhovsky Yu.S., Vigasina M.F., Belakovskiy D.I., Britvin S.N., Sidorov E.G. and Pushcharovsky D.Yu. (2016b) New arsenate minerals from the Arsenatnaya fumarole, Tolbachik volcano, Kamchatka, Russia. VI. Melanarsite, $K_3Cu_7Fe^{3+}O_4(AsO_4)_4$. *Mineralogical Magazine*, **80**, 855–867.

Pekov I.V., Yapaskurt V.O., Belakovskiy D.I., Vigasina M.F., Zubkova N.V. and Sidorov E.G. (2017) New arsenate minerals from the Arsenatnaya fumarole, Tolbachik volcano, Kamchatka, Russia. VII. Pharmazincite, $KZnAsO_4$. *Mineralogical Magazine*, **81**, 1001–1008.

Pekov I.V., Koshlyakova N.N., Belakovskiy D.I., Vigasina M.F., Zubkova N.V., Agakhanov A.A., Britvin S.N., Sidorov E.G. and Pushcharovsky D.Y. (2018a) Paraberzeliite, IMA 2018-001. CNMNC Newsletter No 43, June 2018, page 780. *Mineralogical Magazine*, **82**, 779–785.

Pekov I.V., Koshlyakova N.N., Zubkova N.V., Lykova I.S., Britvin S.N., Yapaskurt V.O., Agakhanov A.A., Shchipalkina N.V., Turchkova A.G. and Sidorov E.G. (2018b) Fumarolic arsenates – a special type of arsenic mineralization. *European Journal of Mineralogy*, **30**, 305–322.

Pekov I.V., Zubkova N.V., Agakhanov A.A., Yapaskurt V.O., Chukanov N.V., Belakovskiy D.I., Sidorov E.G. and Pushcharovsky D.Yu. (2018c) New arsenate minerals from the Arsenatnaya fumarole, Tolbachik volcano,

Kamchatka, Russia. VIII. Arsenowagnerite, $Mg_2(AsO_4)F$. *Mineralogical Magazine*, **82**, 877–888.

Pekov I.V., Zubkova N.V., Agakhanov A.A., Belakovskiy D.I., Vigasina M.F., Yapaskurt V.O., Sidorov E.G., Britvin S.N. and Pushcharovsky D.Y. (2019a) New arsenate minerals from the Arsenatnaya fumarole, Tolbachik volcano, Kamchatka, Russia. IX. Arsenatrotitanite, $NaTiO(AsO_4)$. *Mineralogical Magazine*, **83**, 453–458.

Pekov I.V., Zubkova N.V., Agakhanov A.A., Ksenofontov D.A., Pautov L.A., Sidorov E.G., Britvin S.N., Vigasina M.F. and Pushcharovsky D.Yu. (2019b) New arsenate minerals from the Arsenatnaya fumarole, Tolbachik volcano, Kamchatka, Russia. X. Edtollite, $K_2NaCu_5Fe^{3+}O_2(AsO_4)_4$, and alumoedtollite, $K_2NaCu_5AlO_2(AsO_4)_4$. *Mineralogical Magazine*, **83**, 485–495.

Pekov I.V., Lykova I.S., Yapaskurt V.O., Belakovskiy D.I., Turchkova A.G., Britvin S.N., Sidorov E.G. and Scheidl K.S. (2019c) New arsenate minerals from the Arsenatnaya fumarole, Tolbachik volcano, Kamchatka, Russia. XI. Anatolyite, $Na_6(Ca,Na)(Mg,Fe^{3+})_3Al(AsO_4)_6$. *Mineralogical Magazine*, **83**, 633–638.

Pekov I.V., Lykova I.S., Agakhanov A.A., Belakovskiy D.I., Vigasina M.F., Britvin S.N., Turchkova A.G., Sidorov E.G. and Scheidl K.S. (2019d) New arsenate minerals from the Arsenatnaya fumarole, Tolbachik volcano, Kamchatka, Russia. XII. Zubkovaite, $Ca_3Cu_3(AsO_4)_4$. *Mineralogical Magazine*, **83**, 879–886.

Pekov I.V., Zubkova N.V., Koshlyakova N.N., Agakhanov A.A., Belakovskiy D.I., Vigasina M.F., Yapaskurt V.O., Britvin S.N., Turchkova A.G., Sidorov E.G. and Pushcharovsky D.Y. (2020a) New arsenate minerals from the Arsenatnaya fumarole, Tolbachik volcano, Kamchatka, Russia. XIII. Pansnerite, $K_3Na_3Fe_6^{3+}(AsO_4)_8$. *Mineralogical Magazine*, **84**, 143–151.

Pekov I.V., Koshlyakova N.N., Agakhanov A.A., Zubkova N.V., Belakovskiy D.I., Vigasina M.F., Turchkova A.G., Sidorov E.G. and Pushcharovsky D.Yu. (2020b) New arsenate minerals from the Arsenatnaya fumarole, Tolbachik volcano, Kamchatka, Russia. XIV. Badalovite, $NaNaMg(MgFe^{3+})(AsO_4)_3$, a member of the alluaudite group. *Mineralogical Magazine*, **84**, 616–622.

Pekov I.V., Koshlyakova N.N., Agakhanov A.A., Zubkova N.V., Belakovskiy D.I., Vigasina M.F., Turchkova A.G., Sidorov E.G., Pushcharovsky D.Yu. (2021a) New arsenate minerals from the Arsenatnaya fumarole, Tolbachik volcano, Kamchatka, Russia. XV. Calciojohillerite, $NaCaMgMg_2(AsO_4)_3$, a member of the alluaudite group. *Mineralogical Magazine*, **85**, 215–223.

Pekov I.V., Zubkova N.V., Agakhanov A.A., Yapaskurt V.O., Belakovskiy D.I., Vigasina M.F., Britvin S.N., Turchkova A.G., Sidorov E.G. and Pushcharovsky D.Yu. (2021b) New arsenate minerals from the Arsenatnaya fumarole, Tolbachik volcano, Kamchatka, Russia. XVI. Yurgensonite, $K_2SnTiO_2(AsO_4)_2$, the first natural tin arsenate, and the katiarsite–yurgensonite isomorphous series. *Mineralogical Magazine*, **85**, 698–707.

Shchipalkina N.V., Pekov I.V., Koshlyakova N.N., Britvin S.N., Zubkova N.V., Varlamov D.A. and Sidorov E.G. (2020) Unusual silicate mineralization in fumarolic sublimates of the Tolbachik volcano, Kamchatka, Russia – Part 1: Neso-, cyclo-, ino- and phyllosilicates. *European Journal of Mineralogy*, **32**, 101–119.

Sheldrick G.M. (2015) Crystal structure refinement with SHELXL. *Acta Crystallographica*, **C71**, 3–8.

Symonds R.B. and Reed M.H. (1993) Calculation of multicomponent chemical equilibria in gas-solid-liquid systems: calculation methods, thermochemical data, and applications to studies of high-temperature volcanic gases with examples from Mount St. Helens. *American Journal of Science*, **293**, 758–864.

Tait K.T. and Hawthorne F.C. (2003) Refinement of the crystal structure of arseniopleite: confirmation of its status as a valid species. *The Canadian Mineralogist*, **41**, 71–77.

https://doi.org/10.1180/mgm.2021.82 Published online by Cambridge University Press